Non uniform grids for PDE in finance*

J. Bodeau, G. Riboulet & T. Roncalli

Groupe de Recherche Opérationnelle
Crédit Lyonnais
France

December 15, 2000

Abstract

In this paper, the authors consider non uniform grids to solve PDE in finance. The origin of the problem comes of the fact that computing value-at-risk every day is time-consuming when several options are priced with finite difference methods. One of solution is then to use smaller discretization points. In this case, non uniform grids can then be used to solve PDE with better accuracy than uniform grids. First a solution algorithm is derived and consistency and stability issues are considererd. Then different applications to option pricing are presented. Finally, the problem of stability is studied.

1 Introduction

Probability theory, finance and numerical analysis are the main tools when pricing contingent claims. Fundamental theorems based on no-arbitrage assumptions of asset pricing provide us with a powerful methodology, called the martingale approach, to price any financial product. Indeed, a price could be expressed as an expectation of the discounted payoff under a suitable probability measure (e.m.m.). Thanks to the Feynman-Kac theorem this price could be equally explicited as the solution of a particular backward partial differential equation (PDE). Thus, the famous Black-Scholes formula has been derived by solving a one-dimensional parabolic PDE analogous to the heat equation. Since this breakthrough, PDEs have been playing an ever-increasing role in finance. Indeed, although options could be priced using only the probabilistic approch via Monte-Carlo and lattice methods, it is often faster and more accurate to look for a solution of the differential problem. Solving the PDE may be all the more legitimate as one may be interested in the computation of hedging ratios such as the delta or the gamma.

This paper focuses on how to solve that differential problem using a general finite difference method. The finite difference method is usually implemented with uniform mesh. But, as it is mentionned in Tavella and Randall [2000], it may be useful to adapt the grid to the payoff of the option. It means that when the price of an option may be more sensitive in a precise area, it seems legitimate to concentrate the mesh in that area. Such an approach needs to get an intuitive idea of the "ideal" mesh since one may propose ex-ante the distribution of the discretization points of the grid. It appears that for pricing financial products, one could easily guess where the mesh has to focus on.

This paper is organized as follows. In section two, we present the general algorithm of the finite difference method for non uniform grids. We may also give some arguments about the consistency and the stability of that numerical algorithm. Section three allows to deal with the case where the grids are also non uniform in time. Section four may present some concrete applications of that algorithm to the pricing of options. In

*Views expressed in this paper are the authors' and not those of the Crédit Lyonnais.

particular, we will propose different kinds of grid generations and observe their main advantages and drawbacks when payoffs vary. Finally in section five, one may draw some attention to the case where using non uniform grids could lead to stability problems.

2 Solving partial differential equations with finite difference methods and non uniform grids

We consider the linear parabolic equation

$$\frac{\partial u(t,x)}{\partial t} + c(t,x)\,u(t,x) = \mathcal{A}_t u(t,x) + d(t,x) \tag{1}$$

where $\mathcal{A}_t$ is the general differential operator

$$\mathcal{A}_t u(t,x) = a(t,x)\frac{\partial^2 u(t,x)}{\partial x^2} + b(t,x)\frac{\partial u(t,x)}{\partial x} \tag{2}$$

The main idea is to solve the equation (1) for $(t,x) \in \mathfrak{T} \times \mathfrak{X}$. For convenient computation, we take $\mathfrak{T} = [t^-, t^+]$ and $\mathfrak{X} = [x^-, x^+]$. In this case, we use the method of finite difference, well-adapted for 2-order parabolic equations in x.

2.1 The finite difference method

We introduce a non uniform finite-difference mesh for t and x. Let M and N be be the number of discretisation points for t and x respectively. We note u_i^m be the approximate solution to (1) at the grid point (t_m, x_i) and $u(t_m, x_i)$ the exact solution of the partial differential equation at this point[1]. We use also the notation $h_i = x_i - x_{i-1}$ and $k_m = t_m - t_{m-1}$.

2.1.1 Discretisation scheme for the space

If we consider the central difference method to approximate the derivatives, we have

$$\frac{\partial u(t_m, x_i)}{\partial x} \simeq \frac{u_{i+1}^m - u_{i-1}^m}{x_{i+1} - x_{i-1}} \tag{3}$$

For the second derivative, we suppose that

$$\frac{\partial^2 u(t,x)}{\partial x^2} \simeq h_i^+ \left(u_{i+1}^m - u_i^m\right) - h_i^- \left(u_i^m - u_{i-1}^m\right) \tag{4}$$

For example, we have

$$\begin{aligned} u(t_m, x_{i+1}) &= u(t_m, x_i) + h_{i+1}\frac{\partial u(t_m, x_i)}{\partial x} + \frac{1}{2}h_{i+1}^2\frac{\partial^2 u(t_m, x_i)}{\partial x^2} + O\left(h_{i+1}^3\right) \\ u(t_m, x_{i-1}) &= u(t_m, x_i) - h_i\frac{\partial u(t_m, x_i)}{\partial x} + \frac{1}{2}h_i^2\frac{\partial^2 u(t_m, x_i)}{\partial x^2} + O\left(h_i^3\right) \end{aligned} \tag{5}$$

[1] Nevertheless, $u(t_m, x_i)$ will also denote the approximation solution when we will study the consistency and stability of the algorithm.

It comes that[2]

$$\begin{aligned}\frac{\partial^2 u(t_m,x_i)}{\partial x^2} &= 2\frac{h_i\left(u_{i+1}^m-u_i^m\right)+h_{i+1}\left(u_{i-1}^m-u_i^m\right)}{h_ih_{i+1}^2+h_{i+1}h_i^2}\\ &= 2\frac{h_i\left(u_{i+1}^m-u_i^m\right)-h_{i+1}\left(u_i^m-u_{i-1}^m\right)}{h_ih_{i+1}\left(h_{i+1}+h_i\right)}\end{aligned} \tag{8}$$

and we have

$$\begin{aligned}h_i^+ &= \frac{2}{h_{i+1}\left(h_{i+1}+h_i\right)}\\ h_i^- &= \frac{2}{h_i\left(h_{i+1}+h_i\right)}\end{aligned} \tag{9}$$

The equation (1) becomes

$$\frac{\partial u(t,x)}{\partial t}+c_i^mu_i^m=\mathbf{A}_i^m+d_i^m \tag{10}$$

with

$$\mathbf{A}_i^m=a_i^m\left[h_i^+\left(u_{i+1}^m-u_i^m\right)-h_i^-\left(u_i^m-u_{i-1}^m\right)\right]+b_i^m\frac{u_{i+1}^m-u_{i-1}^m}{x_{i+1}-x_{i-1}} \tag{11}$$

We obtain finally

$$\frac{\partial u(t,x)}{\partial t}=\mathbf{B}_i^m \tag{12}$$

with

$$\mathbf{B}_i^m=\mathbf{A}_i^m+d_i^m-c_i^mu_i^m \tag{13}$$

2.1.2 Discretisation scheme for the time

The most classical method to solve the equation (1) is to use the Euler scheme. We have

$$\frac{\partial u(t,x)}{\partial t}\simeq\frac{u_i^m-u_i^{m-1}}{k_m} \tag{14}$$

We remark also that the equation (1) becomes

$$\frac{u_i^m-u_i^{m-1}}{k_m}+c_i^mu_i^m=\mathcal{A}_lu(t,x)+d_i^m \tag{15}$$

[2] Another approximation could be defined from (5). We have

$$\begin{aligned}\frac{\partial^2 u(t_m,x_i)}{\partial x^2} &\simeq 2\frac{u_{i+1}^m-2u_i^m+u_{i-1}^m-\left(\frac{h_{i+1}-h_i}{h_{i+1}+h_i}\right)\left(u_{i+1}^m-u_{i-1}^m\right)}{h_{i+1}^2+h_i^2}\\ &= 4\frac{h_i\left(u_{i+1}^m-u_i^m\right)-h_{i+1}\left(u_i^m-u_{i-1}^m\right)}{\left(h_{i+1}^2+h_i^2\right)\left(h_{i+1}+h_i\right)}\end{aligned} \tag{6}$$

In this case, we have

$$\begin{aligned}h_i^+ &= 4\frac{h_i}{\left(h_{i+1}^2+h_i^2\right)\left(h_{i+1}+h_i\right)}\\ h_i^- &= 4\frac{h_{i+1}}{\left(h_{i+1}^2+h_i^2\right)\left(h_{i+1}+h_i\right)}\end{aligned} \tag{7}$$

However, the function $\mathcal{A}_t u(t,x)$ depends both on the time t and the space x. That's why we could not employ the traditional Euler algorithm

$$u_i^m = u_i^{m-1} + k_m \left[\mathcal{A}_t u(t,x) + d_i^m - c_i^m u_i^m\right] \tag{16}$$

In this case, we then replace the function $\mathcal{A}_t u(t,x)$ by its numerical approximation $\mathbf{A}_i^m$. So, we have

$$\begin{aligned} u_i^m &= u_i^{m-1} + k_m \left[\mathbf{A}_i^m + d_i^m - c_i^m u_i^m\right] \\ &= u_i^{m-1} + k_m \mathbf{B}_i^m \end{aligned} \tag{17}$$

2.1.3 The θ-scheme method

In the previous paragraph, we have used the single-sided forward difference to approximate the derivative $\frac{\partial u(t,x)}{\partial t}$. There exists another algorithm, like the Richardson extrapolation. The θ-scheme method is a combination of left-sided and right-sided differences. Let $\theta \in [0,1]$. We have

$$u_i^m = u_i^{m-1} + k_m \left[(1-\theta)\,\mathbf{B}_i^{m-1} + \theta \mathbf{B}_i^m\right] \tag{18}$$

Using the expression of $\mathbf{B}_i^m$, we obtain

$$\begin{aligned} u_{i-1}^{m-1}\left[a_i^{m-1}(1-\theta)\,k_m h_i^- - b_i^{m-1}(1-\theta)\frac{k_m}{h_{i+1}+h_i}\right] \\ +u_i^{m-1}\left[1 - a_i^{m-1}(1-\theta)\,k_m\left(h_i^+ + h_i^-\right) - c_i^{m-1}(1-\theta)\,k_m\right] \\ +u_{i+1}^{m-1}\left[a_i^{m-1}(1-\theta)\,k_m h_i^+ + b_i^{m-1}(1-\theta)\frac{k_m}{h_{i+1}+h_i}\right] \\ +u_{i-1}^{m}\left[a_i^{m}\theta k_m h_i^- - b_i^{m}\theta\frac{k_m}{h_{i+1}+h_i}\right] \\ +u_{i}^{m}\left[-1 - a_i^{m}\theta k_m\left(h_i^+ + h_i^-\right) - c_i^{m}\theta k_m\right] \\ +u_{i+1}^{m}\left[a_i^{m}\theta k_m h_i^+ + b_i^{m}\theta\frac{k_m}{h_{i+1}+h_i}\right] \end{aligned} = -\left[d_i^{m-1}(1-\theta)\,k_m + d_i^m \theta k_m\right] \tag{19}$$

2.2 The different numerical algorithms

We note now

$$\begin{aligned} \alpha_i^m &= a_i^m h_i^- - \frac{b_i^m}{h_{i+1}+h_i} \\ \beta_i^m &= a_i^m\left(h_i^+ + h_i^-\right) + c_i^m \\ \gamma_i^m &= a_i^m h_i^+ + \frac{b_i^m}{h_{i+1}+h_i} \end{aligned} \tag{20}$$

2.2.1 The explicit scheme

This scheme corresponds to $\theta = 0$. We have then

$$u_i^m = \alpha_i^{m-1} k_m u_{i-1}^{m-1} + \left(1 - \beta_i^{m-1} k_m\right) u_i^{m-1} + \gamma_i^{m-1} k_m u_{i+1}^{m-1} + d_i^{m-1} k_m \tag{21}$$

We obtain the numerical solution by iterations from the initial condition and by using Dirichlet conditions.

2.2.2 The completely implicit scheme

This scheme corresponds to $\theta = 1$. We have then

$$\alpha_i^m k_m u_{i-1}^m + \left(-1 - \beta_i^m k_m\right) u_i^m + \gamma_i^m k_m u_{i+1}^m = -\left(u_i^{m-1} + d_i^m k_m\right) \tag{22}$$

We obtain the numerical solution by solving the linear system (22) and using Neumann conditions.

2.2.3 The mixed schemes

We have then $\theta \in]0,1[$. For example, the well-famous Crank-Nicholson scheme corresponds to $\theta = \frac{1}{2}$. We introduce the following notations

$$\begin{aligned}
\varsigma_i^m &= (1-\theta)\, k_m \alpha_i^{m-1} \\
\tau_i^m &= 1-(1-\theta)\, k_m \beta_i^{m-1} \\
\upsilon_i^m &= (1-\theta)\, k_m \gamma_i^{m-1} \\
\phi_i^m &= \theta k_m \alpha_i^m \\
\varphi_i^m &= -1-\theta k_m \beta_i^m \\
\chi_i^m &= \theta k_m \gamma_i^m \\
\psi_i^m &= (1-\theta)\, d_i^{m-1} k_m + \theta d_i^m k_m
\end{aligned} \tag{23}$$

To obtain the numerical solution, we have to solve the linear system

$$\phi_i^m u_{i-1}^m + \varphi_i^m u_i^m + \chi_i^m u_{i+1}^m = -\left[\varsigma_i^m u_{i-1}^{m-1} + \tau_i^m u_i^{m-1} + \upsilon_i^m u_{i+1}^{m-1} + \psi_i^m\right] \tag{24}$$

The corresponding matrix form is

$$\Lambda_m \mathbf{u}_m = -\left[\Xi_{m-1}\mathbf{u}_{m-1} + \Psi_m\right] + \varepsilon_m \tag{25}$$

with

$$\mathbf{u}_m = \begin{bmatrix} u_1^m \\ u_2^m \\ \vdots \\ u_i^m \\ \vdots \\ u_{N-3}^m \\ u_{N-2}^m \end{bmatrix} \tag{26}$$

The Υ_m and Φ_m matrices are defined in the following manner

$$\Lambda_m = \begin{bmatrix} \varphi_1^m & \chi_1^m & 0 & & & \\ \phi_2^m & \varphi_2^m & \chi_2^m & 0 & & \\ \ddots & \ddots & \ddots & \ddots & \ddots & \\ & 0 & \phi_i^m & \varphi_i^m & \chi_i^m & 0 \\ & & \ddots & \ddots & \ddots & \ddots \\ & & & 0 & \phi_{N-2}^m & \varphi_{N-2}^m \end{bmatrix} \tag{27}$$

$$\Xi_m = \begin{bmatrix} \tau_1^m & \upsilon_1^m & 0 & & & \\ \varsigma_2^m & \tau_2^m & \upsilon_2^m & 0 & & \\ \ddots & \ddots & \ddots & \ddots & \ddots & \\ & 0 & \varsigma_i^m & \tau_i^m & \upsilon_i^m & 0 \\ & & \ddots & \ddots & \ddots & \ddots \\ & & & 0 & \varsigma_{N-2}^m & \tau_{N-2}^m \end{bmatrix} \tag{28}$$

ε_m is the *residual absortion vector* (Kurpiel and Roncalli [1999])

$$\varepsilon_m = \begin{bmatrix} -\left(\phi_1^m u_0^m + \varsigma_1^{m-1} u_0^{m-1}\right) \\ 0 \\ \vdots \\ 0 \\ \vdots \\ 0 \\ -\left(\chi_{N-2}^m u_{N-1}^m + \upsilon_{N-2}^{m-1} u_{N-1}^{m-1}\right) \end{bmatrix} \tag{29}$$

2.3 Integrating the boundary conditions

A new form of the system of equations (25) is

$$\Lambda_m \mathbf{u}_m = \mathbf{v}_m + \varepsilon_m \tag{30}$$

with

$$\mathbf{v}_m = -\left[\Xi_{m-1}\mathbf{u}_{m-1} + \Psi_m\right]$$

The use of boundary conditions (Dirichlet or/and Neumann)[3]

$$\begin{aligned} & u\left(t^-, x\right) = u_{(t^-)}\left(x\right) \\ & u\left(t, x^-\right) = u_{(x^-)}\left(t\right) \quad \bigvee \quad \left.\frac{\partial\, u\left(t,x\right)}{\partial\, x}\right|_{x=x^-} = u'_{(x^-)}\left(t\right) \\ & u\left(t, x^+\right) = u_{(x^+)}\left(t\right) \quad \bigvee \quad \left.\frac{\partial\, u\left(t,x\right)}{\partial\, x}\right|_{x=x^+} = u'_{(x^+)}\left(t\right) \end{aligned} \tag{31}$$

leads us to modify[4] the equation (30)

$$\Lambda_m^\star \mathbf{u}_m = \mathbf{v}_m^\star \tag{32}$$

with

$$\begin{aligned} \Lambda_m^\star &\longleftarrow \Lambda_m \\ \mathbf{v}_m^\star &\longleftarrow \mathbf{v}_m \\ \left(\mathbf{v}_m^\star\right)_1 &\longleftarrow -\varsigma_1^{m-1} u_0^{m-1} \\ \left(\mathbf{v}_m^\star\right)_{N-1} &\longleftarrow -\upsilon_{N-2}^{m-1} u_{N-1}^{m-1} \end{aligned}$$

- Conditions on x^-
  - Dirichlet: $u\left(t, x^-\right) = u_{x^-}\left(t\right)$

$$\left(\mathbf{v}_m^\star\right)_1 \longleftarrow -\phi_1^m u_{x^-}\left(t_m\right)$$

[3] We introduce the following notations: $\bigvee$ corresponds to the xor operator ($a \bigvee b$ means that only one expression is true — a or b) and $\bigwedge$ is the and operator (with $a \bigwedge b$, both the two expressions a and b are satisfied).

[4] $\longleftarrow$ is an accumulator like the C assignment operator $+=$, i.e. we have

$$a \leftarrow b \Longleftrightarrow a = a + b$$

– Neumann: $\left.\frac{\partial u(t,x)}{\partial x}\right|_{x=x^-} = u'_{x^-}(t)$

$$\begin{aligned}(\Lambda^\star_m)_{1,1} &\longleftarrow \phi_1^m \\ (\mathbf{v}^\star_m)_1 &\longleftarrow \phi_1^m u'_{x^-}(t_m)\, h_1\end{aligned}$$

- Conditions on x^+
  - Dirichlet: $u(t,x^+) = u_{x^+}(t)$

$$(\mathbf{v}^\star_m)_{N-2} \longleftarrow -\chi^m_{N-2} u_{x^+}(t_m)$$

  - Neumann: $\left.\frac{\partial u(t,x)}{\partial x}\right|_{x=x^+} = u'_{x^+}(t)$

$$\begin{aligned}(\Lambda^\star_m)_{N-2,N-2} &\longleftarrow \chi^m_{N-2} \\ (\mathbf{v}^\star_m)_{N-2} &\longleftarrow -\chi^m_{N-2} u'_{x^+}(t_m)\, h_{N-1}\end{aligned}$$

2.4 Consistency and stability

In this paragraph, we give some results about the consistency and stability of the θ-scheme with non uniform grids.

2.4.1 Consistency of numerical approximations

We consider a regular solution of the problem. We are going to show that the numerical approximations in time and space are both consitent. For the first derivative, their order is one. Nevertheless, for the second derivative in space, the order is one and not two like for uniform grids.

- With our numerical scheme, we obtain

$$u(t_m + k_{m+1}, x_i) = u(t_m, x_i) + k_{m+1}\frac{\partial u(t_m,x_i)}{\partial t} + \frac{1}{2}k^2_{m+1}\frac{\partial^2 u(t,x_i)}{\partial t^2} \tag{33}$$

where $t \in [t_m, t_m + k_{m+1}]$. It comes that

$$\left|\frac{u(t_m + k_{m+1}, x_i) - u(t_m, x_i)}{k_{m+1}} - \frac{\partial u(t_m,x_i)}{\partial t}\right| \leq \frac{1}{2}k_{m+1}\left|\frac{\partial^2 u(t,x_i)}{\partial t^2}\right| \tag{34}$$

Let us denote $\mathbf{C}_1 = \max_{t\in[t^-,t^+]}\left|\frac{\partial^2 u(t,x_i)}{\partial t^2}\right|$ and $k = \max k_{m+1}$. We finally have

$$\left|\frac{u(t_m + k_{m+1}, x_i) - u(t_m, x_i)}{k_{m+1}} - \frac{\partial u(t_m,x_i)}{\partial t}\right| \leq \frac{1}{2}\mathbf{C}_1 k \tag{35}$$

- For the first derivative in space, we obtain:

$$\left|\frac{u(t_m, x_i + h_{i+1}) - u(t_m, x_i - h_i)}{h_{i+1} + h_i} - \frac{\partial u(t_m,x_i)}{\partial x}\right| \leq \frac{1}{2(h_{i+1}+h_i)}\left|h^2_{i+1}\frac{\partial^2 u\left(t_m, x_{(+)}\right)}{\partial x^2} - h^2_i\frac{\partial^2 u\left(t_m, x_{(-)}\right)}{\partial x^2}\right| \tag{36}$$

where $x_{(-)} \in [x_i - h_i, x_i]$ and $x_{(+)} \in [x_i, x_i + h_{i+1}]$. We introduce the notation $h = h_i \vee h_{i+1}$. It comes that

$$\left|h^2_{i+1}\frac{\partial^2 u\left(t_m, x_{(+)}\right)}{\partial x^2} - h^2_i\frac{\partial^2 u\left(t_m, x_{(-)}\right)}{\partial x^2}\right| \leq 2\mathbf{C}_2 h^2 \tag{37}$$

where $\mathbf{C}_2 = \max_{x\in\left[x_{(-)},x_{(+)}\right]}\left|\frac{\partial^2 u(t,x)}{\partial x^2}\right|$. We finally obtain

$$\left|\frac{u\left(t_m, x_i + h_{i+1}\right) - u\left(t_m, x_i - h_i\right)}{h_{i+1} + h_i} - \frac{\partial u\left(t_m, x_i\right)}{\partial x}\right| \leq \mathbf{C}_2 h \tag{38}$$

- With a similar analysis, we are going to study consistency for the second derivative in space. By using Taylor formula, we obtain

$$\begin{aligned} u\left(t_m, x_i + h_{i+1}\right) &= u\left(t_m, x_i\right) + h_{i+1}\frac{\partial u\left(t_m, x_i\right)}{\partial x} + \frac{1}{2}h_{i+1}^2\frac{\partial^2 u\left(t_m, x_i\right)}{\partial x^2} + \frac{1}{6}h_{i+1}^3\frac{\partial^3 u\left(t_m, x_{(+)}\right)}{\partial x^3} \\ u\left(t_m, x_i - h_i\right) &= u\left(t_m, x_i\right) - h_i\frac{\partial u\left(t_m, x_i\right)}{\partial x} + \frac{1}{2}h_i^2\frac{\partial^2 u\left(t_m, x_i\right)}{\partial x^2} - \frac{1}{6}h_i^3\frac{\partial^3 u\left(t_m, x_{(-)}\right)}{\partial x^3} \end{aligned} \tag{39}$$

where[5] $x_{(-)} \in [x_i - h_i, x_i]$ and $x_{(+)} \in [x_i, x_i + h_{i+1}]$. We consider the discretisation scheme (9) for the space. It comes that

$$\begin{aligned} h_i^+\left[u\left(t_m, x_{i+1}\right) - u\left(t_m, x_i\right)\right] - h_i^-\left[u\left(t_m, x_i\right) - u\left(t_m, x_{i-1}\right)\right] &= \frac{\partial^2 u\left(t_m, x_i\right)}{\partial x^2} \\ &+ \frac{1}{3\left(h_{i+1} + h_i\right)}\left[h_{i+1}^2\frac{\partial^3 u\left(t, x_{(+)}\right)}{\partial x^3} - h_i^2\frac{\partial^3 u\left(t, x_{(-)}\right)}{\partial x^3}\right] \end{aligned} \tag{40}$$

We have

$$\left|h_{i+1}^2\frac{\partial^3 u\left(t, x_{(+)}\right)}{\partial x^3} - h_i^2\frac{\partial^3 u\left(t, x_{(-)}\right)}{\partial x^3}\right| \leq 2h^2 \max_{x\in\left[x_{(-)},x_{(+)}\right]}\left|\frac{\partial^3 u\left(t, x\right)}{\partial x^3}\right| \tag{41}$$

Let us denote $\mathbf{C}_3 = \max_{x\in\left[x_{(-)},x_{(+)}\right]}\left|\frac{\partial^3 u(t,x)}{\partial x^3}\right|$. We have

$$\left|h_i^+\left[u\left(t_m, x_{i+1}\right) - u\left(t_m, x_i\right)\right] - h_i^-\left[u\left(t_m, x_i\right) - u\left(t_m, x_{i-1}\right)\right] - \frac{\partial^2 u\left(t_m, x_i\right)}{\partial x^2}\right| \leq \frac{2}{3}\mathbf{C}_3 h \tag{42}$$

2.4.2 Consistency of the $\theta-$scheme

We can now study the consitency for the $\theta-$scheme. As for the previous paragraph, we consider a regular solution of the problem and we apply it to our scheme. By Taylor formula, we obtain

$$\frac{u\left(t_m + k_{m+1}, x_i\right) - u\left(t_m, x_i\right)}{k_{m+1}} - \frac{\partial u\left(t_m, x_i\right)}{\partial t} = \frac{1}{2}k_{m+1}\frac{\partial^2 u\left(t_m, x_i\right)}{\partial t^2} + O\left(k_{m+1}^2\right) \tag{43}$$

Because of the order one of the numerical approximation of the second derivative in space, we have

$$h_i^+\left[u\left(t_m, x_{i+1}\right) - u\left(t_m, x_i\right)\right] - h_i^-\left[u\left(t_m, x_i\right) - u\left(t_m, x_{i-1}\right)\right] = \frac{\partial^2 u\left(t_m, x_i\right)}{\partial x^2} + O\left(h\right) \tag{44}$$

We recall that

$$u_i^{m+1} = u_i^m + k_{m+1}\left[\theta\mathbf{B}_i^{m+1} + (1-\theta)\mathbf{B}_i^m\right] \tag{45}$$

Using equations (43) and (44), it comes that

$$\frac{\partial u\left(t_m, x_i\right)}{\partial t} + \frac{1}{2}k_{m+1}\frac{\partial^2 u\left(t_m, x_i\right)}{\partial t^2} + O\left(k_{m+1}^2\right) - \theta\mathbf{B}_i^{m+1} - (1-\theta)\mathbf{B}_i^m = 0 \tag{46}$$

[5] Note that $x_{(-)}$ and $x_{(+)}$ take different values from the previous ones.

with[6]

$$\mathbf{B}_i^m = a(t_m,x_i)\left(\frac{\partial^2 u(t_m,x_i)}{\partial x^2}+O(h)\right)+b(t_m,x_i)\left(\frac{\partial u(t_m,x_i)}{\partial x}+O(h)\right)+ \quad (47)$$

$$d(t_m,x_i)-c(t_m,x_i)u(t_m,x_i) \quad (48)$$

After collecting terms and using the fact that u is the solution of the linear parabolic equation (1), we have[7]

$$\frac{1}{2}k_{m+1}\frac{\partial^2 u(t_m,x_i)}{\partial t^2}+\theta\left(\tilde{\mathbf{B}}_i^m-\tilde{\mathbf{B}}_i^{m+1}\right)+O\left(k_{m+1}^2\right)-a(t_m,x_i)O(h)-b(t_m,x_i)O(h)$$
$$-\theta O(h)\left[a(t_{m+1},x_i)-a(t_m,x_i)+b(t_{m+1},x_i)-b(t_m,x_i)\right] = 0 \quad (49)$$

In the case where the functions a, b, c and d have no time dependence, we obtain

$$\frac{1}{2}k_{m+1}\frac{\partial^2 u(t_m,x_i)}{\partial t^2}-\theta\Delta\tilde{\mathbf{B}}_i^{m+1}+O\left(k_{m+1}^2\right)-a(x_i)O(h)-b(x_i)O(h)=0 \quad (50)$$

with

$$\Delta\tilde{\mathbf{B}}_i^{m+1} = a(x_i)\left(\frac{\partial^2 u(t_{m+1},x_i)}{\partial x^2}-\frac{\partial^2 u(t_m,x_i)}{\partial x^2}\right)+b(x_i)\left(\frac{\partial u(t_{m+1},x_i)}{\partial x}-\frac{\partial u(t_m,x_i)}{\partial x}\right)$$
$$-c(x_i)\left(u(t_{m+1},x_i)-u(t_m,x_i)\right) \quad (51)$$

Using the Taylor formula to first order[8] gives us

$$\frac{1}{2}k_{m+1}\left[\frac{\partial^2 u(t_m,x_i)}{\partial t^2}-2\theta\left(a(x_i)\frac{\partial^3 u(t_m,x_i)}{\partial t\,\partial x^2}+b(x_i)\frac{\partial^2 u(t_m,x_i)}{\partial t\,\partial x}-c(x_i)\frac{\partial u(t_m,x_i)}{\partial t}\right)\right]$$
$$-\theta\left[a(x_i)O\left(k_{m+1}^2\right)+b(x_i)O\left(k_{m+1}^2\right)-c(x_i)O\left(k_{m+1}^2\right)\right]+O\left(k_{m+1}^2\right)-a(x_i)O(h)-b(x_i)O(h) = 0 \quad (53)$$

If we derive in time the linear parabolic equation (1), we have

$$\frac{\partial^2 u(t,x)}{\partial t^2}-\left[a(x)\frac{\partial^3 u(t,x)}{\partial t\,\partial x^2}+b(x)\frac{\partial^2 u(t,x)}{\partial t\,\partial x}-c(x)\frac{\partial u(t,x)}{\partial t}\right]=0 \quad (54)$$

We conclude that in the case where $\theta=\frac{1}{2}$ and the functions a, b, c and d have no time dependance, **the scheme is consistent and its order is two in time and one in space:**

$$\left|u_i^{m+1}-u_i^m-k_{m+1}\left[\theta\mathbf{B}_i^{m+1}+(1-\theta)\mathbf{B}_i^m\right]\right|\leq O\left(k_{m+1}^2\right)+O(h) \quad (55)$$

[6] because we have shown previously that the order of the numerical approximation of the first and second derivative in space is both one.

[7] We use the notation

$$\tilde{\mathbf{B}}_i^m=\mathbf{B}_i^m-a(t_m,x_i)O(h)-b(t_m,x_i)O(h)$$

[8] that is we use the following approximations

$$\frac{\partial^2 u(t_{m+1},x_i)}{\partial x^2}-\frac{\partial^2 u(t_m,x_i)}{\partial x^2} = k_{m+1}\frac{\partial^3 u(t_m,x_i)}{\partial t\,\partial x^2}+O\left(k_{m+1}^2\right)$$
$$\frac{\partial u(t_{m+1},x_i)}{\partial x}-\frac{\partial u(t_m,x_i)}{\partial x} = k_{m+1}\frac{\partial^2 u(t_m,x_i)}{\partial t\,\partial x}+O\left(k_{m+1}^2\right)$$
$$u(t_{m+1},x_i)-u(t_m,x_i) = k_{m+1}\frac{\partial u(t_m,x_i)}{\partial t}+O\left(k_{m+1}^2\right) \quad (52)$$

2.4.3 Stability of the numerical algorithm

We begin to recall the principal theorem of stability in the case of non uniform grids:

Theorem 1 (Thomée [1990]) *The stability property is verified if*

$$k \to 0 \bigwedge h \to 0 \bigwedge r \to 0 \tag{56}$$

where $r = kh^{-2}$ denotes the mesh ratio.

Remark 2 *This is the more general result on stability. But for specific examples, we can obtain more precise results. For example, in the case of the Heat equation, the θ-scheme is* ***unconditionally*** *stable if $\theta \geq \frac{1}{2}$. If $\theta < \frac{1}{2}$, the stability condition becomes $r \leq \frac{1}{2(1-2\theta)}$.*

In this paragraph, we show how non uniform grids modify these results. In particular, we try to exhibit some sufficient conditions for the numerical algorithms to be stable in the particular case of the Heat equations. Thus, we consider the following Dirichlet problem

$$\begin{array}{rcl} \dfrac{\partial u(t,x)}{\partial t} & = & \dfrac{\partial^2 u(t,x)}{\partial x^2} \\ u(0,x) & = & u_0(x) \\ u(t,x_-) & = & u(t,x_+) = 0 \end{array}$$

The discretization method presented above leads to the θ-scheme system presented in the equation (18), i.e

$$A(\theta)\,\mathbf{u}^m = A(\theta - 1)\,\mathbf{u}^{m-1} \tag{57}$$

where

$$\mathbf{u}_m = \begin{bmatrix} u_1^m \\ u_2^m \\ \vdots \\ u_i^m \\ \vdots \\ u_{N-3}^m \\ u_{N-2}^m \end{bmatrix} \tag{58}$$

and $A^m(\theta) = Id + \theta k_m \times H \times B$ with

$$H = \begin{bmatrix} \frac{1}{h_1 h_2} & 0 & & & & & \\ 0 & \ddots & \ddots & & & & \\ & \ddots & \ddots & \ddots & & & \\ & & \ddots & \frac{1}{h_i h_{i+1}} & \ddots & & \\ & & & \ddots & \ddots & 0 & \\ & & & & 0 & \frac{1}{h_{N-2} h_{N-1}} & \end{bmatrix} \tag{59}$$

$$B = \begin{bmatrix} 2 & \frac{-2h_1}{h_1+h_2} & 0 & & & \\ \frac{-2h_3}{h_2+h_3} & 2 & \frac{-2h_2}{h_2+h_3} & \ddots & & \\ 0 & \ddots & \ddots & \ddots & \ddots & \\ & \ddots & \frac{-2h_{i+1}}{h_i+h_{i+1}} & 2 & \frac{-2h_i}{h_i+h_{i+1}} & 0 \\ & & \ddots & \ddots & \ddots & \frac{-2h_{N-2}}{h_{N-3}+h_{N-2}} \\ & & & 0 & \frac{-2h_N}{h_{N-2}+h_{N-1}} & 2 \end{bmatrix} \tag{60}$$

This last matrix could be decomposed as follows

$$B = \widetilde{B} + L \tag{61}$$

where

$$\widetilde{B} = \begin{bmatrix} 2 & -1 & 0 & & & \\ -1 & 2 & -1 & \ddots & & \\ 0 & \ddots & \ddots & \ddots & \ddots & \\ & \ddots & -1 & 2 & -1 & 0 \\ & & \ddots & \ddots & \ddots & -1 \\ & & & 0 & -1 & 2 \end{bmatrix} \tag{62}$$

is the usual matrix of the uniform grids case and

$$L = \begin{bmatrix} 0 & \alpha_1 & 0 & & & \\ -\alpha_2 & 0 & & \ddots & & \\ 0 & \ddots & \ddots & \ddots & \ddots & \\ & \ddots & \ddots & 0 & & 0 \\ & & \ddots & \ddots & \ddots & \alpha_{N-2} \\ & & & 0 & -\alpha_{N-1} & 0 \end{bmatrix} \tag{63}$$

with

$$\alpha_i = \frac{h_{i+1} - h_i}{h_i + h_{i+1}} \tag{64}$$

Thus, for instance, in the case of a spatial mesh given by

$$x_i = f\left(\frac{i}{N}\right) \tag{65}$$

with an increasing function $f \in \mathcal{C}^2\left([0,1], [x_-, x_+]\right)$ we have

$$\alpha_i = \frac{C_i}{N} \tag{66}$$

with

$$|C_i| \leq \frac{\sup_{x\in[0,1]} |f''(x)|}{2 \inf_{x\in[0,1]} f'(x)} \tag{67}$$

Moreover, we know that in the following expression

$$A(\theta) = \underbrace{\left(Id + \theta k_m \times H \times \widetilde{B}\right)}_{C(\theta)} + \underbrace{\theta k_m \times H \times L}_{\varepsilon(\theta)} \tag{68}$$

all the eigenvalues λ_i of the the first matrix $C(\theta)$ could be written in the following way

$$\lambda_i = 1 + \theta k_m \nu_i^2 \tag{69}$$

because the eigenvalues of the matrix $\widetilde{B}$ are known to be $4\sin^2\left(\frac{i\pi}{N-1}\right)$ for $i \in \{1, ..., N-2\}$, and the matrix H is diagonal definite positive so that the eigenvalues of the matrix $H \times \widetilde{B}$ are positive and could be written as ν_i^2. Thus, the matrix $C(\theta)$ is always inversible and

$$\|A(\theta) - C(\theta)\|_\infty = \|\varepsilon(\theta)\|_\infty \leq 2k_m \max_i \left|\frac{1}{h_i h_{i+1}}\right| \max_i \left|\frac{h_{i+1} - h_i}{h_i + h_{i+1}}\right| \tag{70}$$

It means that

$$\forall\theta, \quad \exists k_0(\theta) \quad | \, \forall k_m < k_0(\theta) \quad A(\theta) \text{ is inversible}$$

So, $\forall k_m < k_0(\theta)$

$$\mathbf{u}^m = A(\theta)^{-1} A(\theta - 1) \mathbf{u}^{m-1} \tag{71}$$

and

$$\left\|A(\theta)^{-1} A(\theta - 1)\right\|_\infty \leq \frac{\|A(\theta - 1)\|_\infty}{\|A(\theta)\|_\infty} \leq \frac{\|C(\theta - 1)\|_\infty + \|\varepsilon(\theta - 1)\|_\infty}{\|C(\theta)\|_\infty - \|\varepsilon(\theta)\|_\infty} \tag{72}$$

Using (69) the biggest eigenvalue of the matrix $C(\theta)$ is a $1 + \theta k_m \nu_{i^*}^2$ and the biggest eigenvalue of the matrix $C(\theta - 1)$ is a $1 + (\theta - 1) k_m \nu_{i^*}^2$ with the same i^*. So, since they also get the same eigenvector we have

$$\frac{\|C(\theta - 1)\|_\infty}{\|C(\theta)\|_\infty} = \left\|C(\theta)^{-1} C(\theta - 1)\right\|_\infty = \left|\frac{1 + (\theta - 1) k_m \nu_{i^*}^2}{1 + \theta k_m \nu_{i^*}^2}\right|$$

and for $\theta \geq \frac{1}{2}$

$$-1 < \frac{1 + (\theta - 1) k_m \nu_{i^*}^2}{1 + \theta k_m \nu_{i^*}^2} < 1$$

So $\frac{\|C(\theta-1)\|_\infty}{\|C(\theta)\|_\infty} < 1$ and since $\|\varepsilon(\theta - 1)\|_\infty$ and $\|\varepsilon(\theta)\|_\infty$ are respectiveley negligible with respect to$\|C(\theta - 1)\|_\infty$ and $\|C(\theta)\|_\infty$ when $\|\varepsilon(\theta)\|_\infty$ tends to 0, we could conclude that $\left\|A(\theta)^{-1} A(\theta - 1)\right\|_\infty \leq 1$ when $\|\varepsilon(\theta)\|_\infty$ is very small,so that the θ-scheme becomes stable. Finally, we have the following results :

Proposition 3 *In the case of the Heat equation, for a θ-scheme where $\theta \geq \frac{1}{2}$, the numerical algorithm presented above is stable (so is convergent) as soon as*

$$2k_m \max_i \left|\frac{1}{h_i h_{i+1}}\right| \max_i \left|\frac{h_{i+1} - h_i}{h_i + h_{i+1}}\right| \tag{73}$$

is small enough.

Remark 4 *Using the definitions $k = \max k_m$, $h = \max h_i$, $r = \max k_m / (h_i h_{i+1})$, we retry a stability condition*[9] *similar this of the theorem 1.*

[9] Because we deduce from the equation (70) that

$$\|\varepsilon(\theta)\|_\infty \to 0 \tag{74}$$

3 The case of temporal non uniform grids

In the previous analysis, the grid can be non uniform in space, in time or both in space and time. In figure 1, we have represented some examples of non uniform grids. Nevertheless, the grid in x is the same for every value of t_m. In this section, we present a modification of the algorithm in order to use temporal non uniform grids. This type of grids corresponds to figure 2. In this case, we have to introduce a new notation $x_i^{(m)}$ which is the i-th point of the grid at time $t = t_m$. The i-th point $x_i^{(m)}$ is not necessarily the i-th point $x_i^{(m+1)}$ at time $t = t_{m+1}$. Moreover, the number of discretisation points and the boundaries could change with t_m.

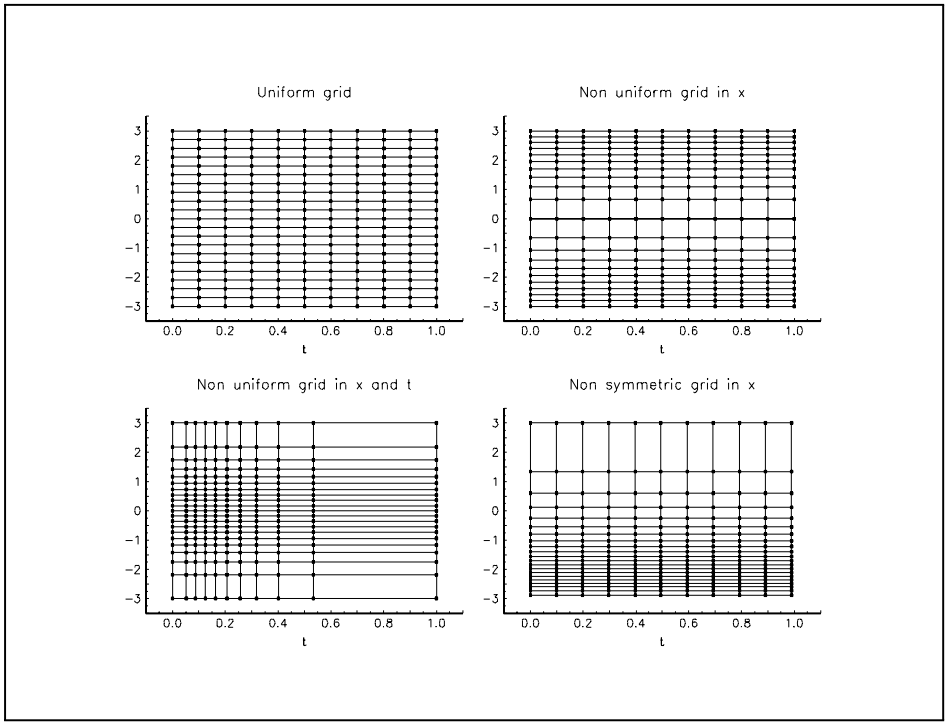

Figure 1: Examples of non-uniform grids

We just present the main ideas to modify the previous algorithm, but we invite the reader to consult the GAUSS code to understand the modifications in a more deaper way. Figure 3 presents the graphical representation of temporal non uniform grids. The problem is that some points (or all points) of the grid $x_i^{(m)}$ could not coincide with the points of the grid $x_i^{(m+1)}$. But solving the equation system (24) for $x_i^{(m+1)}$ requires the numerical solution of $u\left(t_m, x_i^{(m+1)}\right)$ and not of $u\left(t_m, x_i^{(m)}\right)$. The idea is then to 'estimate' the values of $u\left(t_m, x_i^{(m+1)}\right)$ knowing these of $u\left(t_m, x_i^{(m)}\right)$. If we suppose that the solution is regular, this can be achieved by an interpolation method. In our GAUSS code, we have choosen a cubic interpolation method. The numerical solution at t_m is then obtained by solving the following linear system

$$\Lambda_m \mathbf{u}_m = -\left[\Xi_{m-1}\tilde{\mathbf{u}}_{m-1} + \Psi_m\right] + \varepsilon_m \tag{75}$$

where $\tilde{\mathbf{u}}_{m-1}$ is not the numerical solution $\mathbf{u}_{m-1}$ obtained at the previous iteration, but the interpolated values

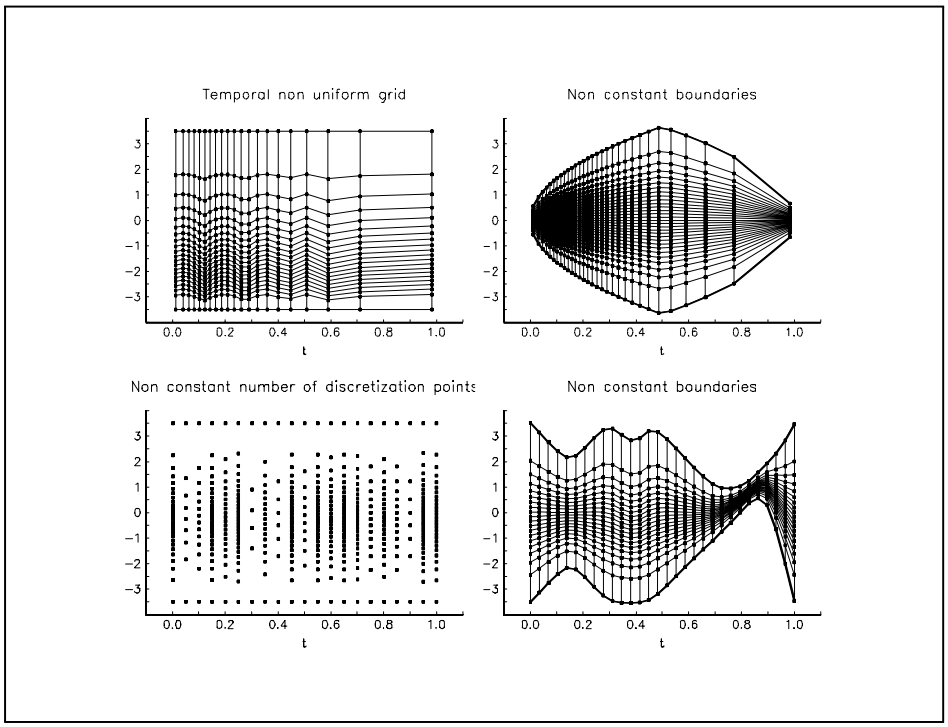

Figure 2: Examples of temporal non-uniform grids

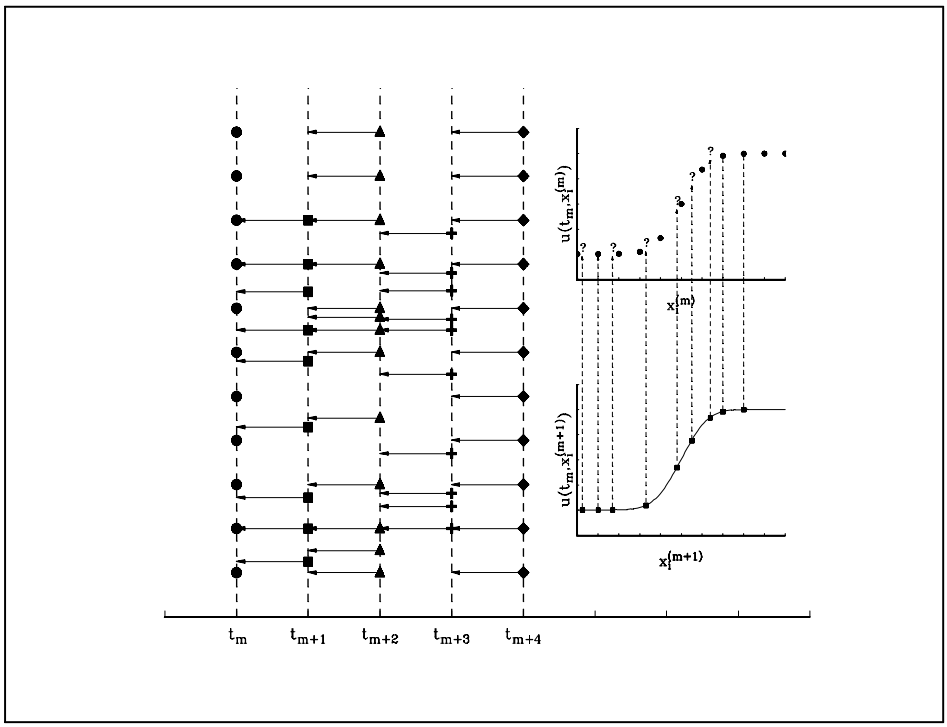

Figure 3: The problem of temporal non-uniform grids

of $\mathbf{u}_{m-1}$ for the vector $\mathbf{x} = \mathbf{x}^{(m)}$of dimension $N^{(m)}$. Here is the iterative process:

$$\begin{array}{ccccccccccc}
\mathbf{u}_0 & \longrightarrow & \tilde{\mathbf{u}}_0 & \longrightarrow & \mathbf{u}_1 & \longrightarrow & \tilde{\mathbf{u}}_1 & \longrightarrow & \mathbf{u}_2 & \longrightarrow & \tilde{\mathbf{u}}_2 & \longrightarrow & \dots \\
\downarrow & & \downarrow & & \downarrow & & \downarrow & & \downarrow & & \downarrow & & \\
\mathbf{x}^{(0)} & & \mathbf{x}^{(1)} & & \mathbf{x}^{(1)} & & \mathbf{x}^{(2)} & & \mathbf{x}^{(2)} & & \mathbf{x}^{(3)} & & \\
N^{(0)} & & N^{(1)} & & N^{(1)} & & N^{(2)} & & N^{(2)} & & N^{(3)} & &
\end{array}$$

4 Some options pricing examples

In this section, we are going to study some particular cases of option pricing where we will compare the results obtained with uniform grids and non uniform grids.

4.1 Non uniform grids generation

To create non uniform grids, we can use different methods to generate the points. We present now three grid generation methods:

1. We note $\mathfrak{G}_1(x^-, x^+, N)$ the uniform grid, that is
$$\mathcal{X} := \{x_i\} = \left\{ x^- : \frac{(x^+ - x^-)}{N-1} : x^+ \right\} \tag{76}$$

2. In the second grid $\mathfrak{G}_2(\mathbf{F}, x^-, x^+, N)$, we consider a probability density function $\mathbf{F}(x)$. As in a sampling procedure, the points $\{x_i\}$ correspond to N realizations of the random variable with distribution $\mathbf{F}$. If we consider a deterministic sampling, we have
$$\mathbf{F}(x_i) - \mathbf{F}(x_{i-1}) = \frac{1}{N} \tag{77}$$

3. The third $\mathfrak{G}_3(x^\star, \alpha, x^-, x^+, N)$ use a transformation which places the points around a target $x^\star$. For example, Tavella and Randall [2000] suggest the following transformation:
$$x_i = x^\star + \alpha \sinh\left(\mathbf{c}_2 \frac{i}{N} + \mathbf{c}_1 \left(1 - \frac{i}{N} \right) \right) \tag{78}$$
where
$$\begin{aligned}
\mathbf{c}_1 &= \sinh^{-1}\left(\frac{x^- - x^\star}{\alpha} \right) \\
\mathbf{c}_2 &= \sinh^{-1}\left(\frac{x^+ - x^\star}{\alpha} \right)
\end{aligned} \tag{79}$$
As explained by Tavella and Randall [2000], "this transformation maps the interval $[0,1]$ to the interval $[x^-, x^+]$ and grid points are therefore concentrated near the critical point $x^\star$". α is a parameter which determines the uniformity of the grid. If α is small, we obtain a highly non uniform grids whereas the grid is uniform for a high value of α

Note that we can generate others non uniform grids by pointwise compound methods. Here are some examples:

$$\begin{aligned}
\mathfrak{G}_4 &= a_1\mathfrak{G}_1\left(x^-, x^+, N\right) + a_2\mathfrak{G}_2\left(\mathbf{F}, x^-, x^+, N\right) + a_3\mathfrak{G}_3\left(x^\star, \alpha, x^-, x^+, N\right) \\
\mathfrak{G}_5 &= a_1\mathfrak{G}_3\left(x_1^\star, \alpha_1, x^-, x^+, N\right) + a_2\mathfrak{G}_3\left(x_2^\star, \alpha_2, x^-, x^+, N\right) \\
\mathfrak{G}_6 &= \sqrt{\mathfrak{G}_1(x^-, x^+, N)\,\mathfrak{G}_3(x^\star, \alpha, x^-, x^+, N)}
\end{aligned} \tag{80}$$

4.2 European options

We introduce some notations. $S(t)$ denotes the price of the underlying asset at time t. We assume that the price $S(t)$ is a geometric brownian motion under the risk-neutral probability $\mathbb{Q}$

$$\left\{ \begin{array}{rcl} \mathrm{d}S(t) & = & bS(t)\,\mathrm{d}t + \sigma S(t)\,\mathrm{d}W(t) \\ S(t_0) & = & S_0 \end{array} \right. \tag{81}$$

with $W(t)$ a $\mathbb{Q}$-Wiener process, b the *cost-of-carry* parameter and σ the volatility. Let us denote $C(t_0, S_0)$ the value of an European call option with strike K and maturity T. $C(t_0, S_0)$ is given by the formula of Black and Scholes [1973]. We may show that the price is the solution of the following PDE

$$\left\{ \begin{array}{l} \frac{1}{2}\sigma^2 S^2 \partial_S^2 C(t,S) + bS\,\partial_S C(t,S) + \partial_t C(t,S) - rC(t,S) = 0 \\ C(T,S) = (S-K)^+ \end{array} \right. \tag{82}$$

We have solved this equation with three grids:

1. The first grid is a uniform grid;
2. The second grid is based on the inversion of the delta greek coefficient[10];
3. The third one corresponds to the Tavella-Randall grids with $x^\star = K$ and $\alpha = 2$.

The parameters take the following numerical values: $K = 100$, $T = 0.25$, $\sigma = 0.2$, $r = 0.05$ and $b = 0$. For the grid generation, we set $x^- = 50$, $x^+ = 150$, $N = 151$ and $M = 251$. We have represented the grids in figure 4. Figure 5 presents the numerical errors. We remark that the non uniform grids give better results for this numerical example.

4.3 American options

The pricing of American options is a problem of stopping time. The exercise of an American option at time τ procures for the holder a payoff $\varrho(\tau, S(\tau))$. The payoff function ϱ is continuous and nonnegative. The option is issued at time $t_0 = 0$ and the expiration date is T. The no arbitrage argument imply that the price of an American option $C(t, S(t))$ verifies at each time t

$$C(t, S(t)) \geq \varrho(t, S(t)) \tag{83}$$

The stopping region is therefore defined as

$$\mathcal{D} = \{(t, S(t)) \in [0,T] \times \mathcal{R}_S \mid C(t, S(t)) = \varrho(t, S(t))\} \tag{84}$$

The continuation region is the complement of $\mathcal{D}$ in $[0,T] \times \mathcal{R}_S$

$$\mathcal{C} = \{(t, S(t)) \in [0,T] \times \mathcal{R}_S \mid C(t, S(t)) > \varrho(t, S(t))\} \tag{85}$$

The stopping boundary is the frontier $\partial\mathcal{C} \subset \mathcal{D}$ of $\mathcal{C}$ expressed in terms of the underlying asset. The optimal stopping time is the first time the underlying asset reaches the stopping boundary. It is thus defined by

$$\begin{array}{rcl} \tau^* & = & \inf\{\tau \in [t,T] \mid C(\tau, S(\tau)) = \varrho(\tau, S(\tau))\} \\ & = & \inf\{\tau \in [t,T] \mid (\tau, S(\tau)) \in \mathcal{D}\} \end{array} \tag{86}$$

The American call price is the solution of a variational inequalities problem:

$$\left\{ \begin{array}{l} \left[\frac{1}{2}\sigma^2 S^2 \partial_S^2 C(t,S) + bS\,\partial_S C(t,S) + \partial_t C(t,S) - rC(t,S)\right](C(t,S) - \varrho(\tau,S)) \leq 0 \\ C(T,S) = \varrho(\tau,S) = (S-K)^+ \end{array} \right. \tag{87}$$

[10] Note that the delta of the call option scaled by $e^{(b-r)\tau}$ is a probability distribution.

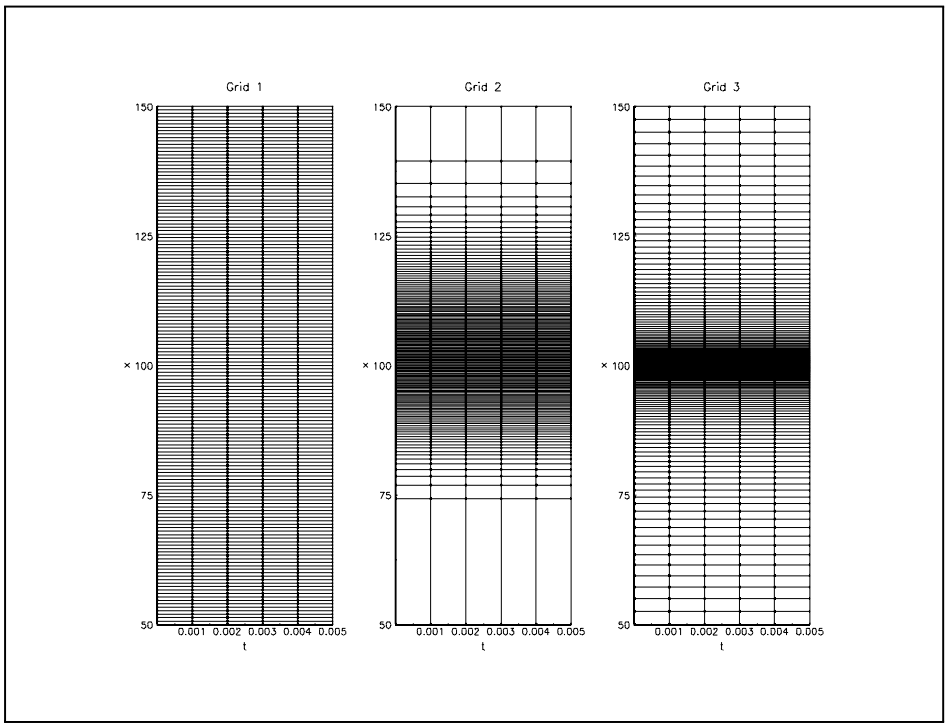

Figure 4: Grids of the European call example

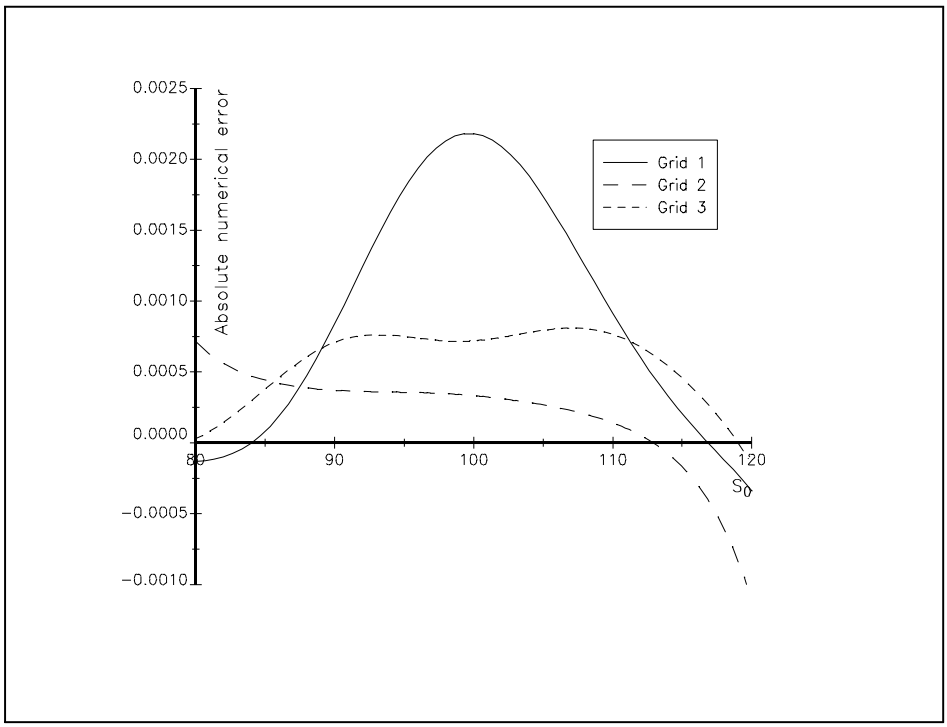

Figure 5: Numerical errors for the European call example

We consider the previous example with the same parameters[11] and we use a fourth grid which is a slight modification of the third grid — $x^\star$ is not equal to the strike, but corresponds to the value 110. Figure 6 represents the stopping region $\mathcal{D} = \{(t, S(t)) \in [0,T] \times \mathcal{R}_S \mid S(t) = S^\star\}$. We remark that non uniform grids give a more smoothed stopping frontier.

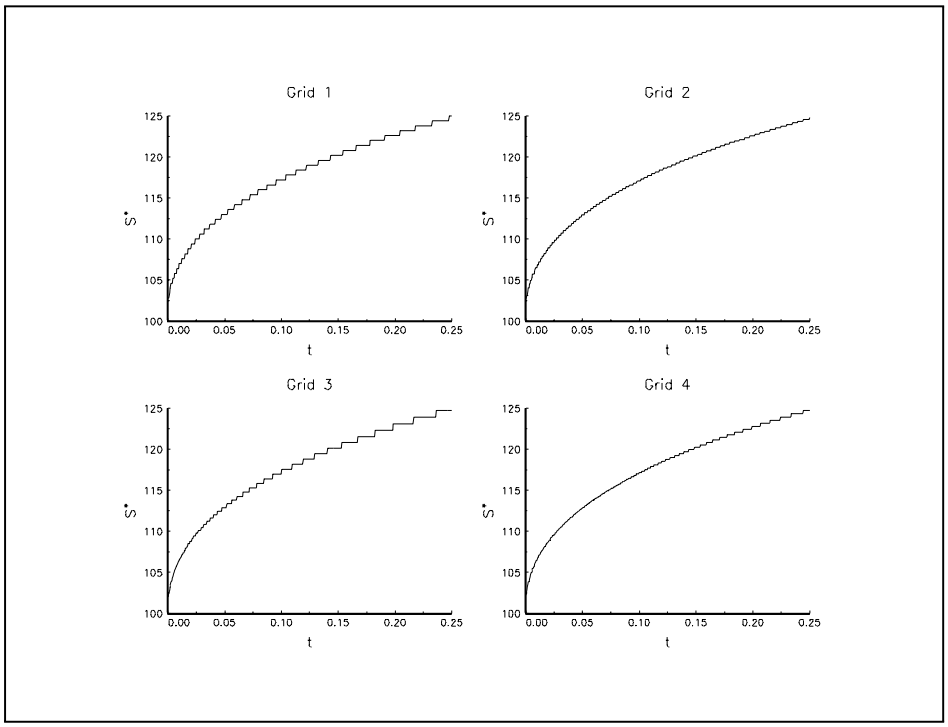

Figure 6: Stopping region of the American call example

4.4 Binary and Barrier options

We consider now the case of exotic options, and in particular binary and barrier options. We use the previous example of the European option, but we change now the payoff function. In the case of the Binary option, the payoff is $\chi_{[S(T)\geq K]}$. We have used the Tavella-Rendall grids with $x^\star = K$ and different values of α. When α is equal to 200, the grid is almost uniform.

We then consider an Up-and-Out call option (UOC) with a barrier L equal to 110 and same parameters. For the non uniform grid, we use the previous Tavella-Rendall grid but with $x^\star = L$. We consider also a temporal non uniform grid defined as follows $\mathfrak{G} = \mathfrak{G}_3(x^\star(t), \alpha(t), x^-, x^+, N)$ with

- $x^\star(t) = L$ and $\alpha(t) = 200$ for $t \in \left[0, \frac{1}{3}T\right]$;
- $x^\star(t) = L$ and $\alpha(t) = 20$ for $t \in \left[\frac{1}{3}T, \frac{2}{3}T\right]$;
- and $x^\star(t) = K$ and $\alpha(t) = 2$ for $t \in \left[\frac{2}{3}T, T\right]$.

[11] However, we set $x^- = 50$, $x^+ = 200$, $N = 251$ and $M = 501$.

Thanks to formulas provided by RUBINSTEIN and REINER [1991], we have computed the absolute error for the price and the greeks. Figure 8 corresponds to the binary option, whereas the errors for the barrier option are shown in figure 7. We remark that non uniform grids may give better results than uniform grids. Moreover, it appears in the case of the barrier option that using a temporal grid can improve the results.

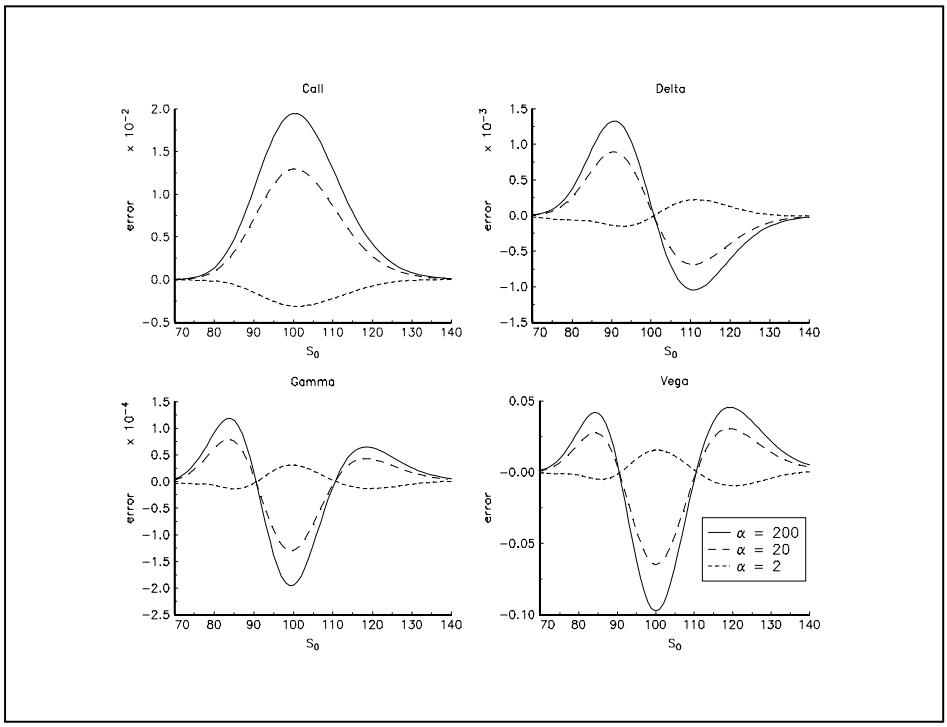

Figure 7: Numerical errors for the Binary call example

5 When non uniform grids do not work?

We have shown that we could obtain better results with a non uniform grids. However, if we analyse the stability equation (**??**), we remark that the expression of the mesh ratio is

$$r_1 = \max \frac{k_m}{h_i^2} \tag{88}$$

In the case of uniform grids with mesh spacings k and h, r_2 is equal to kh^{-2}. With the same number of discretization points, it comes necessarily that $r_1 > r_2$. And in some cases, the non uniform mesh ratio can be very large. We can then face to some stability problems. We have illustrated them in figures 9 and 10. In figure 9, we use the previous example of pricing an European call option both with a uniform grid and a non uniform grid based on the Tavella-Randall method and just modify the number N of points in space. We observe a problem when the price S is close to the strike K in the case of the non uniform grids. This stability problem has a big impact on the computation of the greeks. It can be explained by the fact that $k_m h_i^{-2}$ is very large in this region when N is important. Figure 10 represents the evolution of the mesh ratio with respect to N if the other parameters are given[12]. The difference between uniform and non uniform mesh ratios can be very huge.

[12] We have taken $t^- = 0$, $t^+ = 1$, $M = 51$, $x^- = 50$ and $x^+ = 150$. The grid is the Tavella-Rendall's one with $x^\star = 100$.

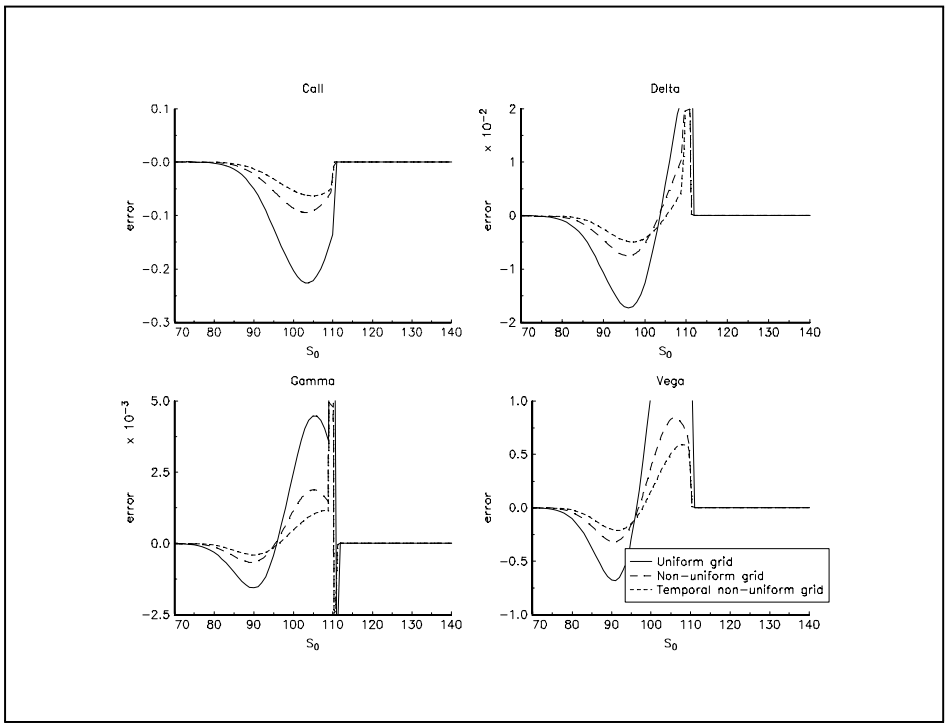

Figure 8: Numerical errors for the Barrier call example

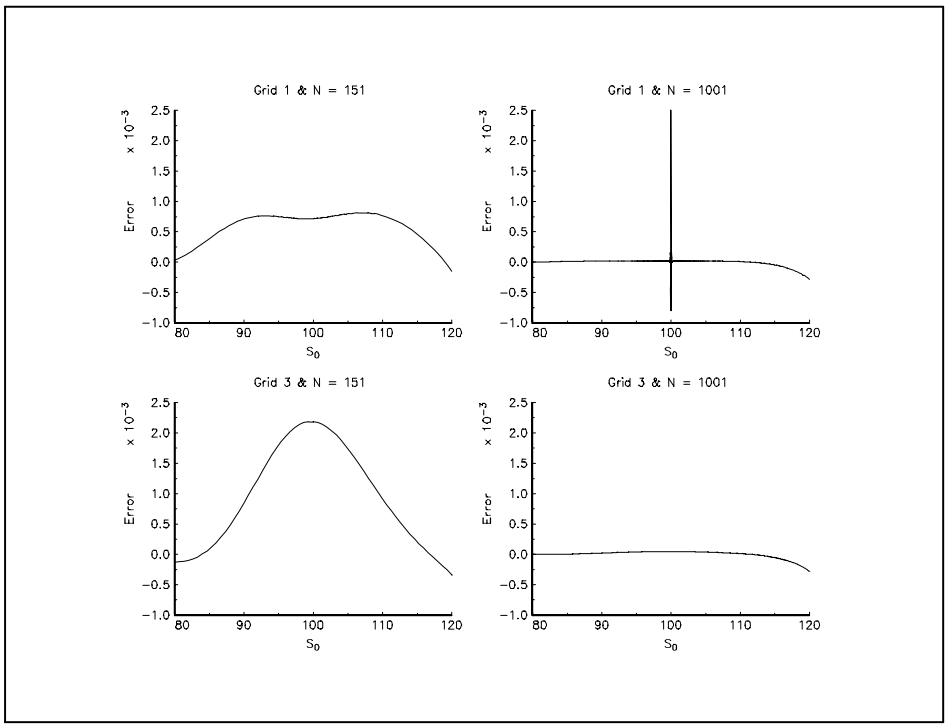

Figure 9: Numerical errors when we increase the discretization number for the space

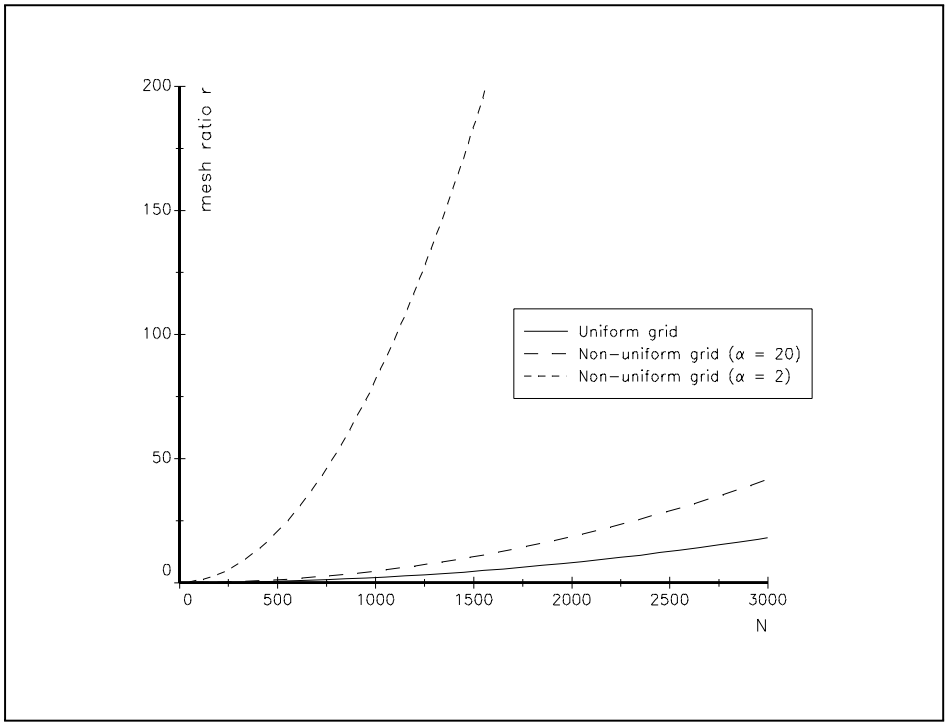

Figure 10: Mesh ratio of uniform grids versus non-uniform grids

6 Conclusion

In this paper, we have proposed the use of non uniform grids to solve PDE problems in finance. We have derived the θ-scheme algorithm and we have considered its stability and consistency. Moreover, we have povided some examples who show the interest of such methods. However, we must be careful with these methods when the number of discretization points is high because they may produce significant errors.

The main advantage of non uniform grids in finance is that we can obtain better results when the number of discretization points is low. It is very interesting in value-at-risk applications. To compute VaR with derivatives, we have to revalue the mark-to-market of the portfolio. Because it is time consuming (when the valuation is done by solving PDEs) and we do not neet greeks, we can use a number of discretization points smaller than the one used by the trader. Non uniform grids can then be useful for that.

In this paper, we have used 'naive' non uniform grids. However, it would be interesting to determine 'optimal' grids. For example, in the case of Barrier options, we can concentrate grid points near the strike K or the barrier L or the price of the asset S_0. We can also construct the grid by mixtures of the three grids. We have

$$a_1 \mathfrak{G}_3\left(K, \alpha_1, S^-, S^+, N\right) + a_2 \mathfrak{G}_3\left(L, \alpha_2, S^-, S^+, N\right) + a_3 \mathfrak{G}_3\left(S_0, \alpha_3, S^-, S^+, N\right) \tag{89}$$

with $a_1 + a_2 + a_3 = 1$. It would be interesting to have an idea about the optimal values of a_1, a_2 and a_3 and α_1, α_2 and α_3 of which minimize the criterion $\left(u\left(t_0, S_0\right) - C\left(t_0, S_0\right)\right)^2$ where $C\left(t_0, S_0\right)$ is the true value. And we can complicate the problem by assuming that the a's and α's are time-dependent. Another example is the Dupire model which is computational intensive. Solving the PDE of Dupire [1994] requires to calibrate the volatility surface $\sigma^2\left(\tau, K\right)$ in each points of the grid. Because the time of computation can then be long[13], we

[13] In fact, it never exceeds few seconds, which is a "long" time when we have to revalue a portfolio with thousands of products.

can suggest to use a non uniform grid. The problem is what grid to use. Perhaps, the 'optimal' grid is not necessarily the same as for the Rubinstein-Reiner model.

Because the grids are determined ex ante, it would be also interesting to have a "rational" procedure which generates the grid depending on the payoff function. We leave this development for later works.

References

[1] Black, F. and M. Scholes [1973], The pricing of options and corporate liabilities, *Journal of Political Economy*, **81**, 637-659

[2] Bodeau, J., G. Riboulet and T. Roncalli [2000], A GAUSS implementation of non uniform grids for pde — the PDE library, Groupe de Recherche Opérationnelle, Crédit Lyonnais

[3] De Boor, C. [1978], A Pratical Guide to Splines, *Applied Mathematical Sciences*, **27**, Springer-Verlag, New York

[4] Dupire, B. [1994], Pricing with a smile, *Risk Magazine*, **7-1**, 18-20

[5] Kurpiel, A. and T. Roncalli [1999], Hopscotch methods for two-state financial models, *Journal of Computational Finance*, **3-2**, 53-89

[6] Rubinstein, M.E. and E. Reiner [1991], Breaking down the barriers, *Risk Magazine*, **4-8**, 28-35

[7] Shikin, E.V. and A.I. Plis [1995], Handbook on Splines (for the User), CRC Press, Boca Raton

[8] Stoer, J. and R. Bulirsch [1993], Introduction to Numerical Analysis, *Texts in Applied Mathematics*, **12**, Springer-Verlag, New York

[9] Tavella, D. and C. Randall [2000], Pricing Financial Instruments — The Finite Difference Method, *Wiley Series In Financial Engineering*, John Wiley & Sons, New York

[10] Thomée, V. [1990], Finite difference methods for linear parabolic equations, in P.G. Ciarlet and J.L. Lions (eds), *Handbook of Numerical Analysis — Volume I*, North-Holland, 5-196

A Cubic spline interpolation

We follow the presentation of Shikin and Plis [1995]. Let the interval $[a, b]$ with the grid ϖ defined by

$$a = x_0 < x_1 < \cdots < x_n = b \tag{90}$$

Definition 5 *A cubic spline $\mathcal{S}_\varpi(x)$ on ϖ is a real function with the properties:*

1. $\mathcal{S}_\varpi(x) \in C^2[a, b]$;
2. $\mathcal{S}_\varpi(x)$ *is a polynomial of order 3 on every segment* $\varpi_i = [x_i, x_{i+1}]$

$$\mathcal{S}_\varpi(x) = \mathcal{S}_i(x) = \alpha_i + \beta_i(x - x_i) + \gamma_i(x - x_i)^2 + \delta_i(x - x_i)^3 \tag{91}$$

In the interpolation problem, we assume that the cubic spline's graph passes through the points (x_i, y_i). We could show that (Stoer and Bulirsch [1993])

$$\begin{aligned}
\alpha_i &= y_i \\
\beta_i &= \left(\frac{y_{i+1} - y_i}{h_{i+1}}\right) - h_{i+1}\left(\frac{\mathcal{S}''_{i+1}(x_{i+1}) + 2\mathcal{S}''_i(x_i)}{6}\right) \\
\gamma_i &= \frac{1}{2}\mathcal{S}''_i(x_i) \\
\delta_i &= \frac{\mathcal{S}''_{i+1}(x_{i+1}) - \mathcal{S}''_i(x_i)}{6h_{i+1}}
\end{aligned} \tag{92}$$

with $h_i = x_i - x_{i+1}$. In order to determine the coefficients of the polynomials, we need two more restrictions, which are generally based on boundary conditions. For example, we could use these two end conditions:

- **End conditions of the first type**

$$\left\{ \begin{array}{rcl} \mathcal{S}'_\varpi(x_0) & = & y'_0 \\ \mathcal{S}'_\varpi(x_n) & = & y'_n \end{array} \right. \tag{93}$$

- **End conditions of the second type**

$$\left\{ \begin{array}{rcl} \mathcal{S}''_\varpi(x_0) & = & 0 \\ \mathcal{S}''_\varpi(x_n) & = & 0 \end{array} \right. \tag{94}$$

Let us define the following scalars

$$\begin{array}{rcl} \lambda_i & = & \dfrac{h_{i+1}}{h_{i+1}+h_i} \\ \mu_i & = & 1-\lambda_i \\ \nu_i & = & \dfrac{6}{h_{i+1}+h_i}\left(\dfrac{y_{i+1}-y_i}{h_{i+1}} - \dfrac{y_i - y_{i-1}}{h_i}\right) \end{array} \tag{95}$$

The cubic spline interpolation requires also to solve the system of the form

$$\left\{ \begin{array}{l} 2z_0 + \lambda_0^\star z_1 = \nu_0^\star \\ \mu_i z_{i-1} + 2z_i + \lambda_i z_{i+1} = \nu_i \qquad i = 1, 2, \ldots, n-1 \\ \mu_n^\star z_{n-1} + 2z_n = \nu_n^\star \end{array} \right.$$

with $z_i := \mathcal{S}''_i(x_i)$. In the case of the second type, we have $\lambda_0^\star = \nu_0^\star = \mu_n^\star = \nu_n^\star = 0$. For the first case, we have $\lambda_0^\star = \mu_n^\star = 1$, $\nu_0^\star = 6h_1^{-1}\left(h_1^{-1}(y_1 - y_0) - y'_0\right)$ and $\nu_n^\star = 6h_n^{-1}\left(y'_n - h_n^{-1}(y_n - y_{n-1})\right)$. Solving the previous system lead us to find the values of α_i, β_i, γ_i and δ_i thanks to the equations (92).

B GAUSS implementation

PDE is a GAUSS implementation of the methods described in this paper. The library and its manual (Bodeau, Riboulet and Roncalli [2000]) can be downloaded at the following url:

http://www.gro.creditlyonnais.fr